**Supplementary Information**

Zhang et al.: A Single-Cell Transcriptomic landscape of Primate Arterial Aging

## Supplementary Figure 1

**a**

| NO. | Gender | Age (year) | Equivalent age range in humans (year) | Number of total cells | Number of filtered cells |
|---|---|---|---|---|---|
| YF1 | Female | 5 | ~18 | 672 | 601 |
| YF2 | Female | 5 | ~18 | 576 | 543 |
| YF3 | Female | 5 | ~18 | 576 | 543 |
| YF4 | Female | 4 | ~14 | 480 | 441 |
| YM1 | Male | 5 | ~18 | 560 | 537 |
| YM2 | Male | 5 | ~18 | 576 | 538 |
| YM3 | Male | 6 | ~21 | 432 | 370 |
| YM4 | Male | 6 | ~21 | 576 | 523 |
| OF1 | Female | 18 | ~63 | 576 | 538 |
| OF2 | Female | 19 | ~67 | 576 | 552 |
| OF3 | Female | 19 | ~67 | 576 | 558 |
| OF4 | Female | 20 | ~70 | 576 | 531 |
| OM1 | Male | 18 | ~63 | 576 | 539 |
| OM2 | Male | 19 | ~67 | 480 | 450 |
| OM3 | Male | 20 | ~70 | 480 | 452 |
| OM4 | Male | 21 | ~74 | 1152 | 949 |

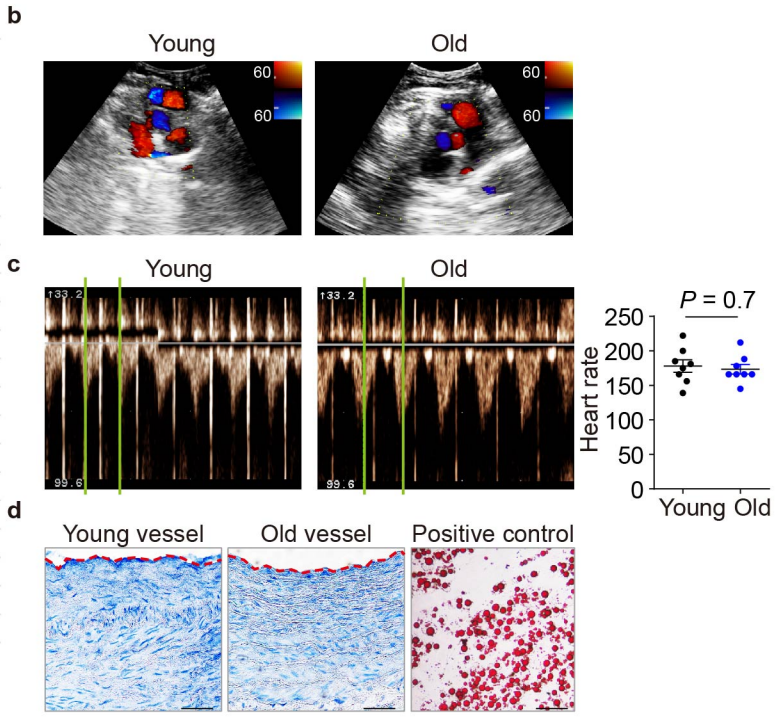


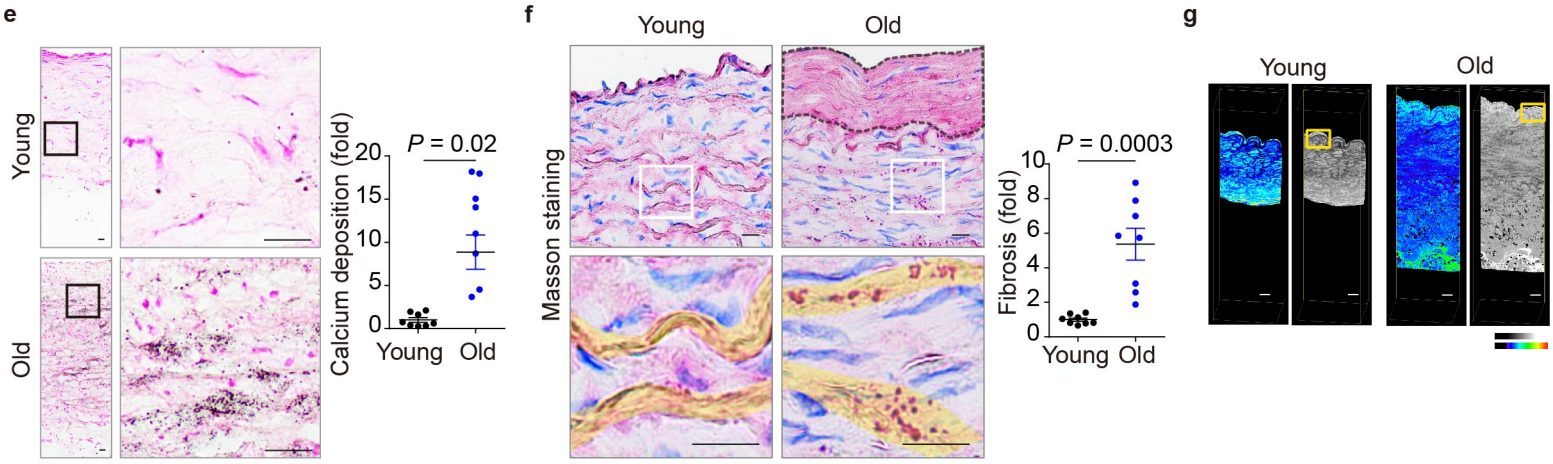

**Supplementary Fig. 1, Information about the monkeys and the single-cell isolation procedure. a,** Characteristics of the monkeys used for these analyses. **b,** Ultrasound-based imaging for visualization of cardiac health in young and old monkeys. Blue and red regions indicate the bloodstream flowing in opposite directions. **c**, Ultrasound-based measurement of heart rate in young and old monkeys. Green vertical line, a beating cycle. **d,** Oil red O staining of monkey vessel tissue and human adipocyte tissue as a positive control. Scale bar, 100 μm. **e,** Deposition of calcium in areas of the vessel wall that were darkly stained with von Kossa in young and old samples (left) and the calculated percentage of the dark area (right). Scale bar, 100 μm. **f**, Left, Sirius Red staining shows aortic morphology; right, relative changes in fibrosis. Yellow areas, fragmented internal elastic lamina; black dashed lines, thickened fiber cap. White squares correspond to the enlarged areas shown in the lower images. Scale bar, 20 μm. **g,** Left, representative section of large-scale three-dimensional reconstruction of a vessel (positioned from the red line). Right, the representative section before coloring with Imaris 9.2.1. Yellow rectangle, the enlarged area shown in the lower right corner of Fig. 1c. n = 8 monkeys (**c, e, f**). Data are the mean ± SEM; p-values were determined by two-tailed Student's t-test (**c, e, f**).

## Supplementary Figure 2

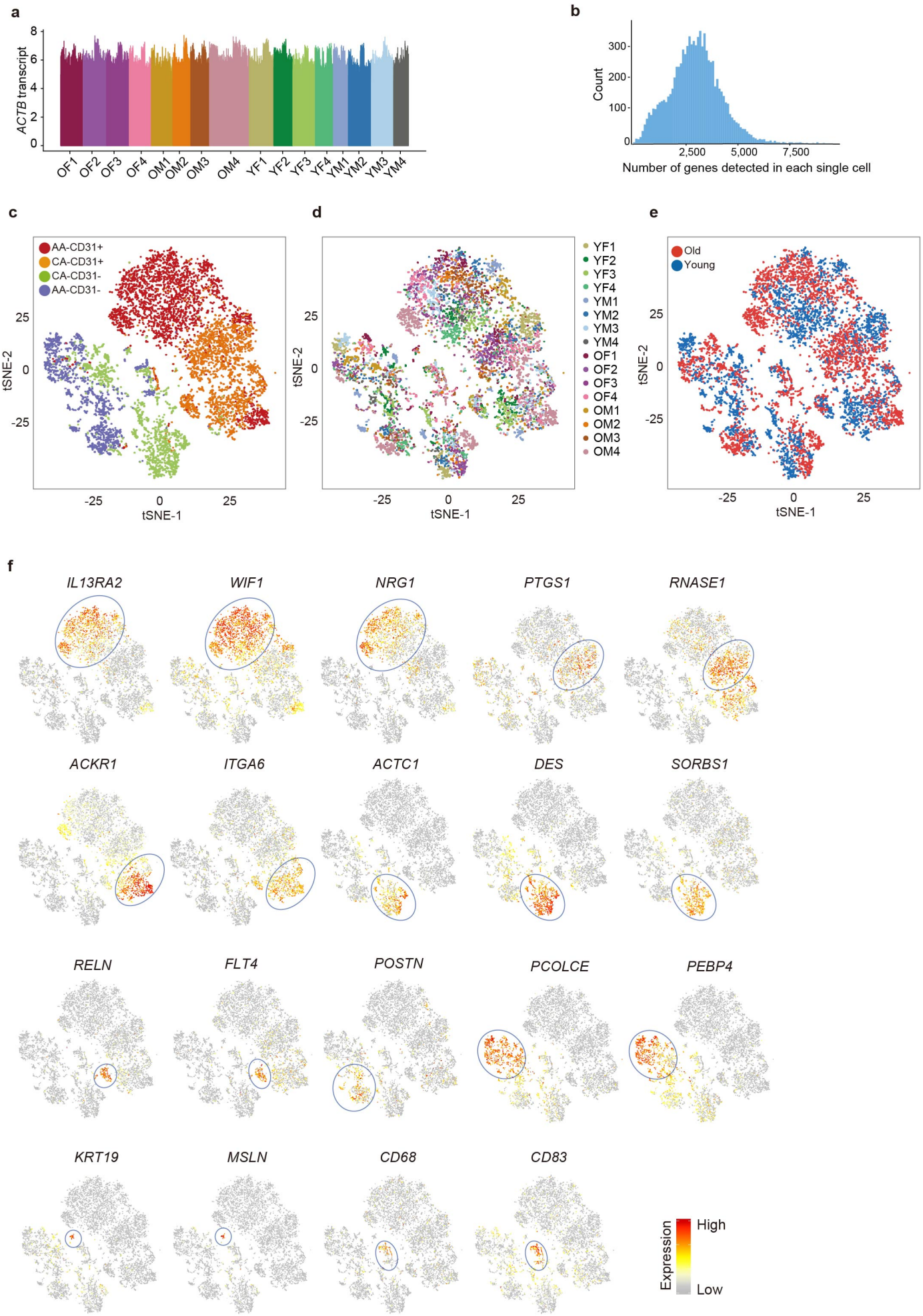

**Supplementary Fig. 2, scRNA-Seq analysis. a,** Expression of *ACTB* in single cells across young and old monkeys. **b,** Binning counts of the number of genes detected in each cell. **c,** Regional surveys. The t-SNE of 7,989 $CD31^+$ and $CD31^-$ cells from the aortic arch (AA) and coronary artery (CA) (n = 16 monkeys) is shown, colored by region and surface markers. **d,** *t*-SNE plots of cells in the aortic arches (AAs) and coronary arteries (CAs). n = 16 monkeys. No obvious differences in distribution were observed among the different batches from different monkeys. Each color represents one monkey. **e,** Age effect surveys. The *t*-SNE of $CD31^+$ and $CD31^-$ cells from the AA and CA (n = 16 monkeys) is shown, color-coded by age. **f,** Expression of known and newly identified cell type-specific markers is shown using the same layout as in Fig. 1f (gray, no expression; dark red, relatively higher expression).

## Supplementary Figure 3

**a**

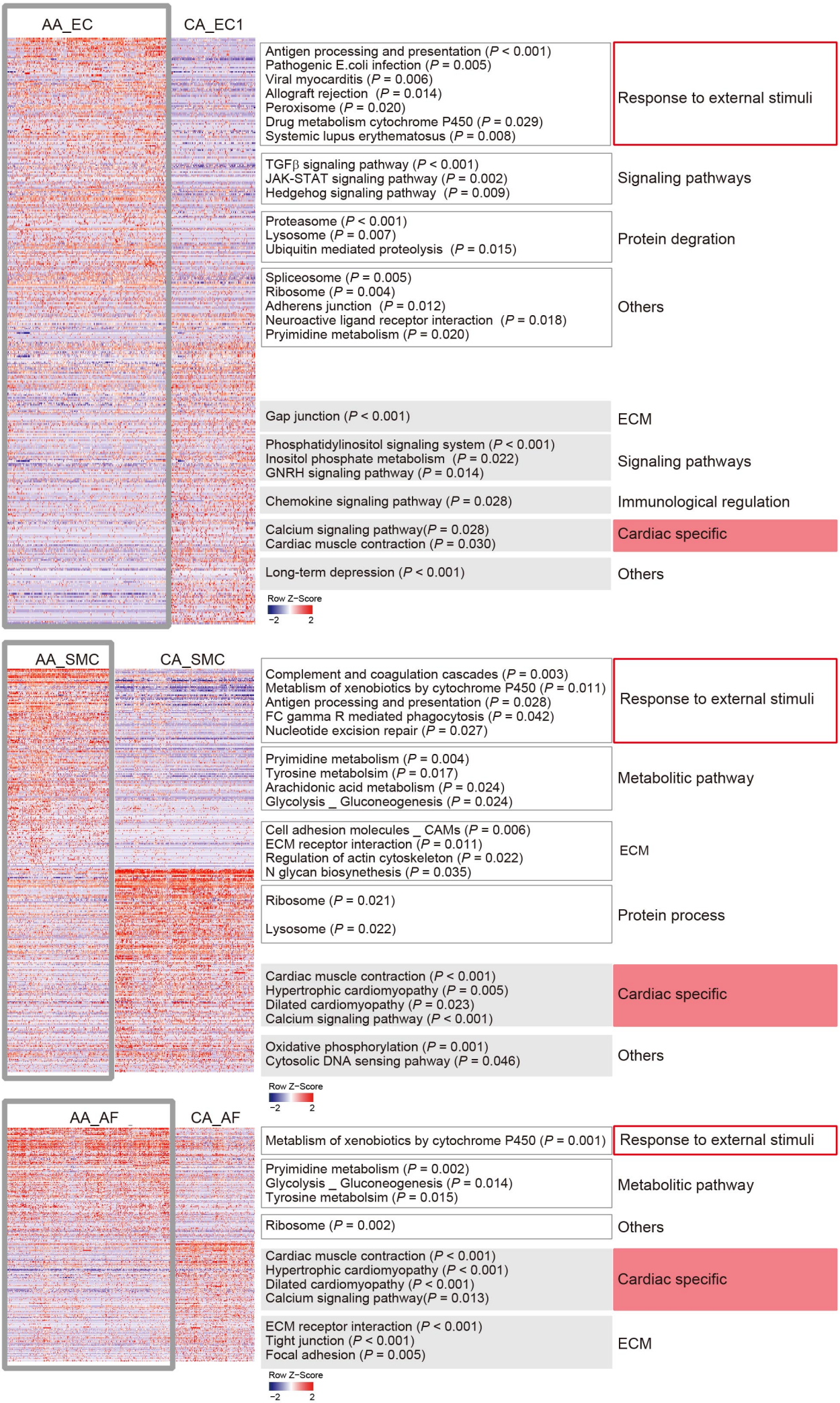

**Supplementary Fig. 3, Zonation principles. a,** Heatmap showing differentially expressed genes between AA_EC and CA_EC1/2, AA_SMC and CA_SMC, and AA_AF and CA_AF; the corresponding pathways identified by GSEA (nominal p-value ≤ 0.05 and FDR ≤ 25%) are labeled on the right. See Fig. 1 for cell type abbreviations.

## Supplementary Figure 4

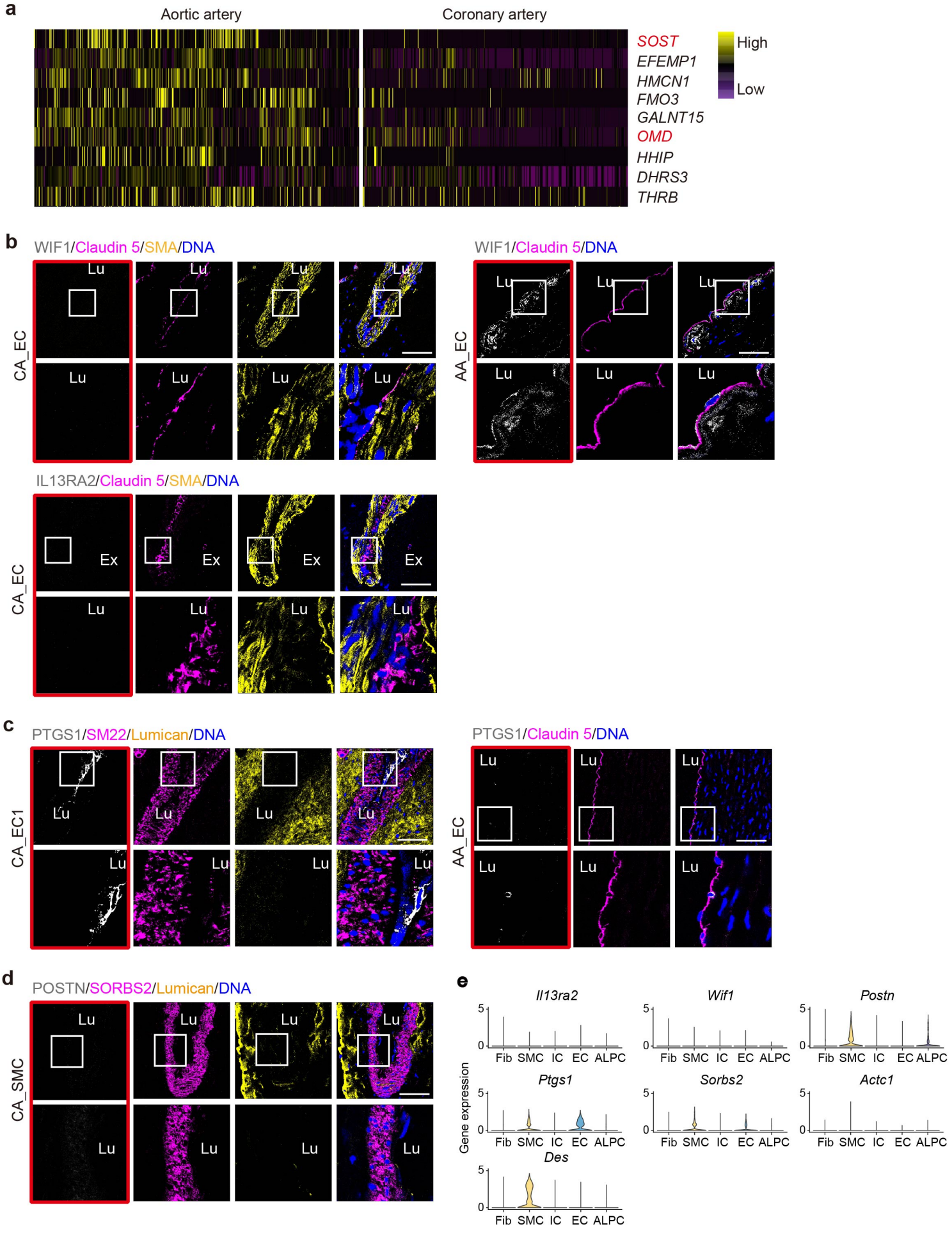

**Supplementary Fig. 4, Immunofluorescence staining of the aortic artery and coronary artery for the indicated markers. a,** Heatmap showing genes that are more highly expressed in aortic ECs, SMCs and fibroblasts than in coronary ECs, SMCs, and fibroblasts. **b,** Immunofluorescence staining shows that *WIF1* and *IL13RA2* (markers for AA_EC) are expressed in endothelial cells from the aortic artery but not in endothelial cells from the coronary artery. See also Fig. 2c. **c,** Immunofluorescence staining shows that *PTGS1* (a marker for CA_EC1) is specifically expressed in endothelial cells from the coronary artery (left) but is rarely expressed in endothelial cells from the aortic artery (right). See also Fig. 2d. **d,** Immunofluorescence staining shows that the absence of *POSTN* (a marker for AA_SMC) in SMCs from the coronary artery. See also Fig. 2e. White squares correspond to enlarged areas shown in the lower images. Lu, lumen; Ex, extravascular space. Scale bar, 50 μm. **e,** Violin plots showing the expression of indicated genes in various cell types of rat aorta. Fib, fibroblasts; SMC, smooth muscle cells; IC, immune cells; EC, endothelial cells; ALPC, aortic-localized proliferative cells.

## Supplementary Figure 5

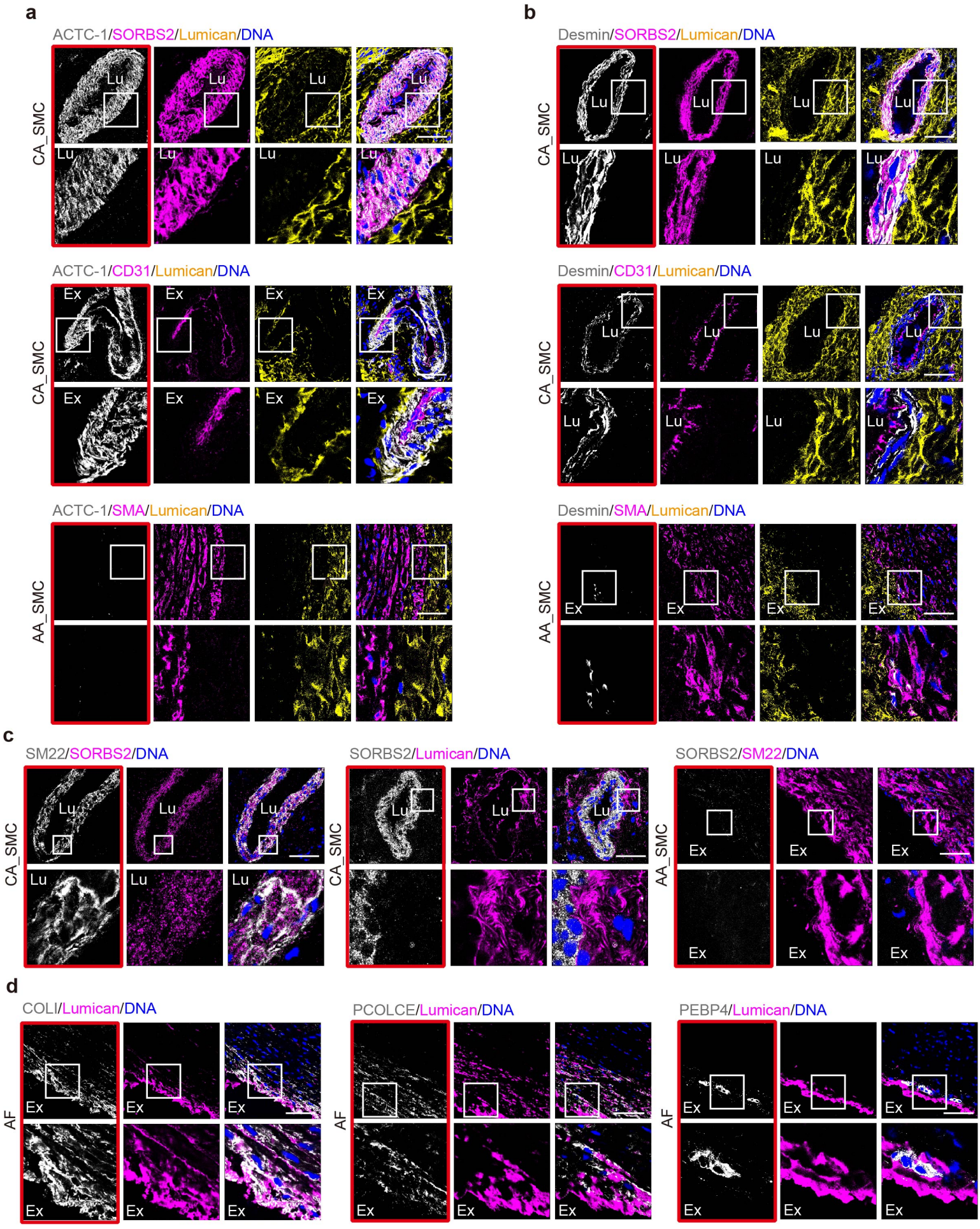

**Supplementary Fig. 5, Immunofluorescence staining of the aortic artery and the coronary artery for the CA_SMC and AF markers. a,** Immunofluorescence staining shows *ACTC-1* (a marker for CA_SMC) expressed in smooth muscle cells from the coronary artery but not in smooth muscle cells from the aortic artery. **b,** Immunofluorescence staining shows *Desmin* (a marker for CA_SMC) expressed in smooth muscle cells from the coronary artery but rarely expressed in smooth muscle cells from the aortic artery. See also Fig. 2f. **c,** Immunofluorescence staining shows *SORBS2* (a marker for CA_SMC) expressed in smooth muscle cells from the coronary artery but not in smooth muscle cells from the aortic artery. See also Fig. 2f. **d,** Immunofluorescence staining shows *COLI*, *PCOLCE*, and *PEBP4* (markers for AF) expressed in adventitial fibroblasts from the aortic artery. White squares correspond to enlarged areas shown in the lower images. Lu, lumen; Ex, extravascular space. Scale bar, 50 μm.

Supplementary Figure 6

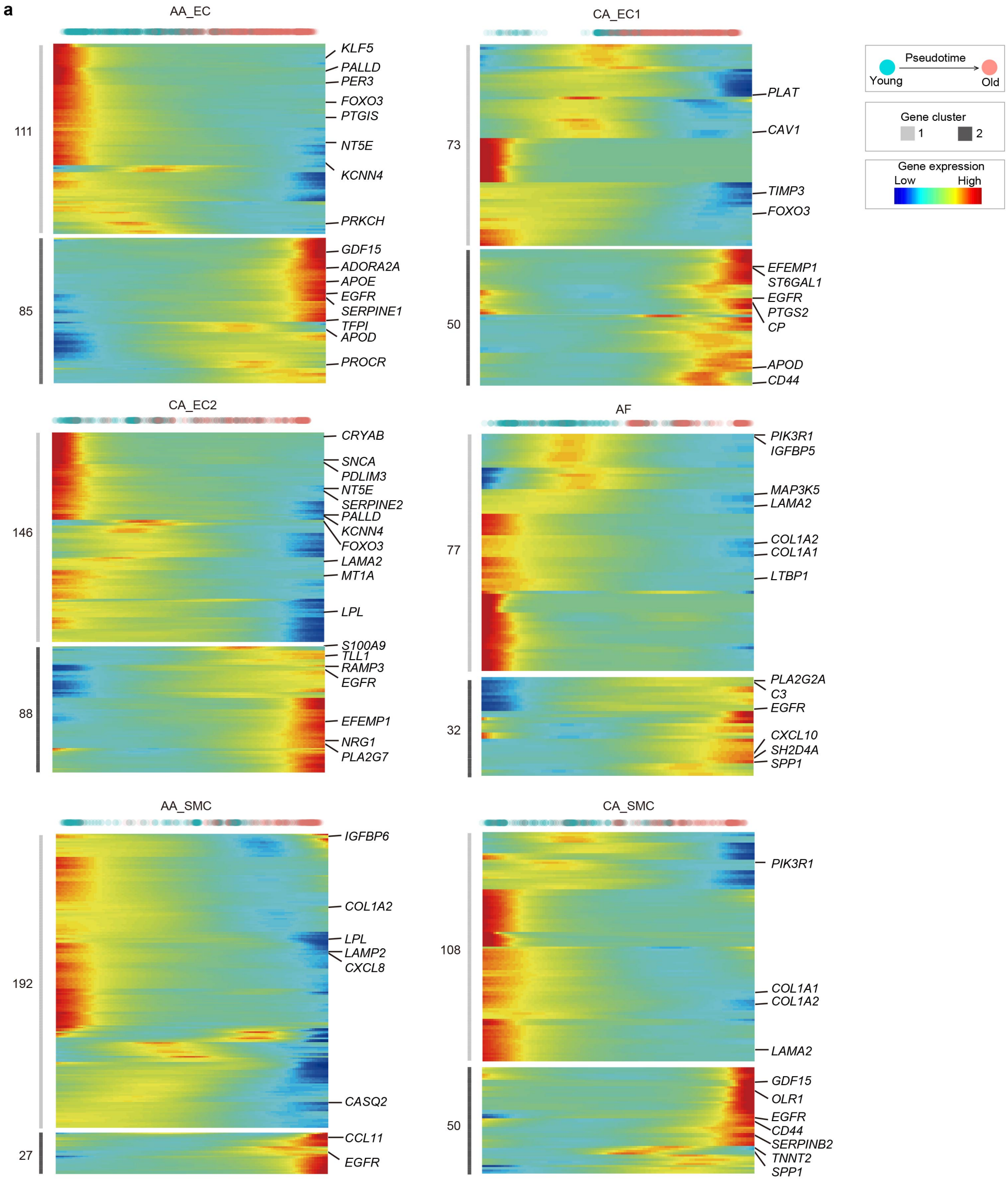

**Supplementary Fig. 6, Relative expression pattern of O/Y DEGs in each cell type. a,** Heatmap of the relative expression (red, high; blue, low) of O/Y DEGs (Bonferroni-corrected p-value ≤ 0.05 and $\log_2$ [fold change] ≥ 0.5) that covaried as individual cell types transitioned from a young state to an old state, as determined by a pseudotime analysis using Monocle2. Cells of each type were ordered across the pseudotime scale shown above the heatmap; cells from young monkeys are blue, and cells from old monkeys are red. See Fig. 1 for cell type abbreviations. O/Y DEGs were clustered in two groups, and the number of genes in each cluster is shown to the left of the heatmap. Genes associated with aging/longevity or cardiovascular disease are shown to the right of each heatmap panel.

Supplementary Figure 7

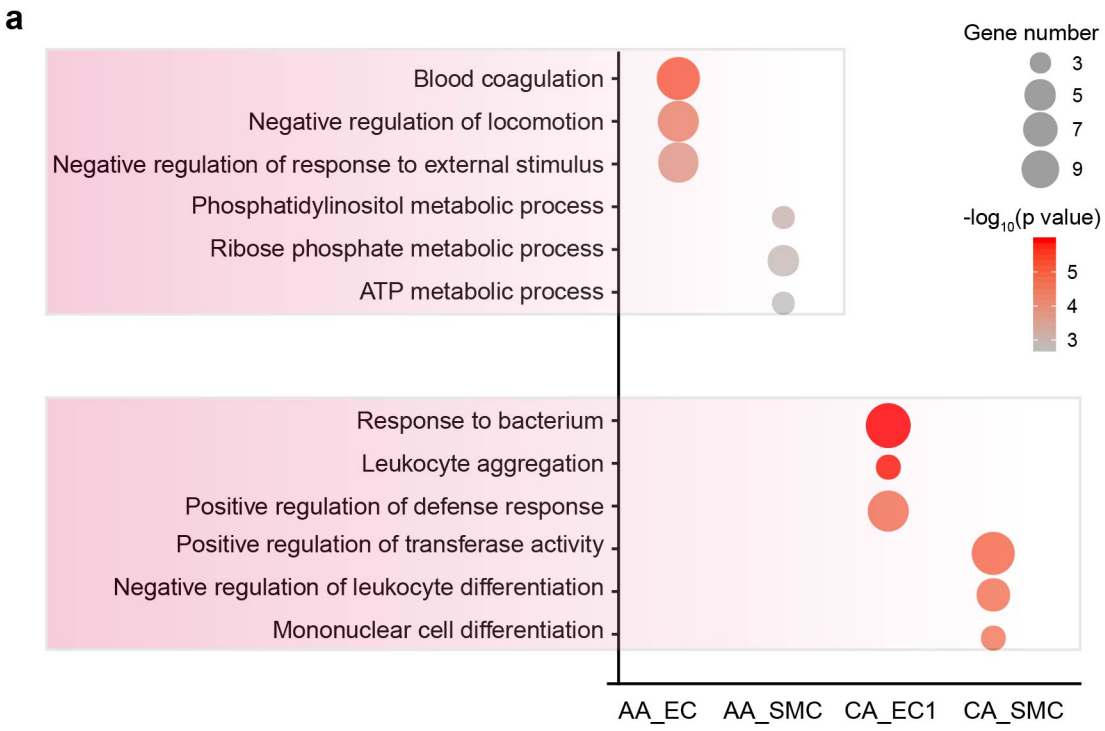


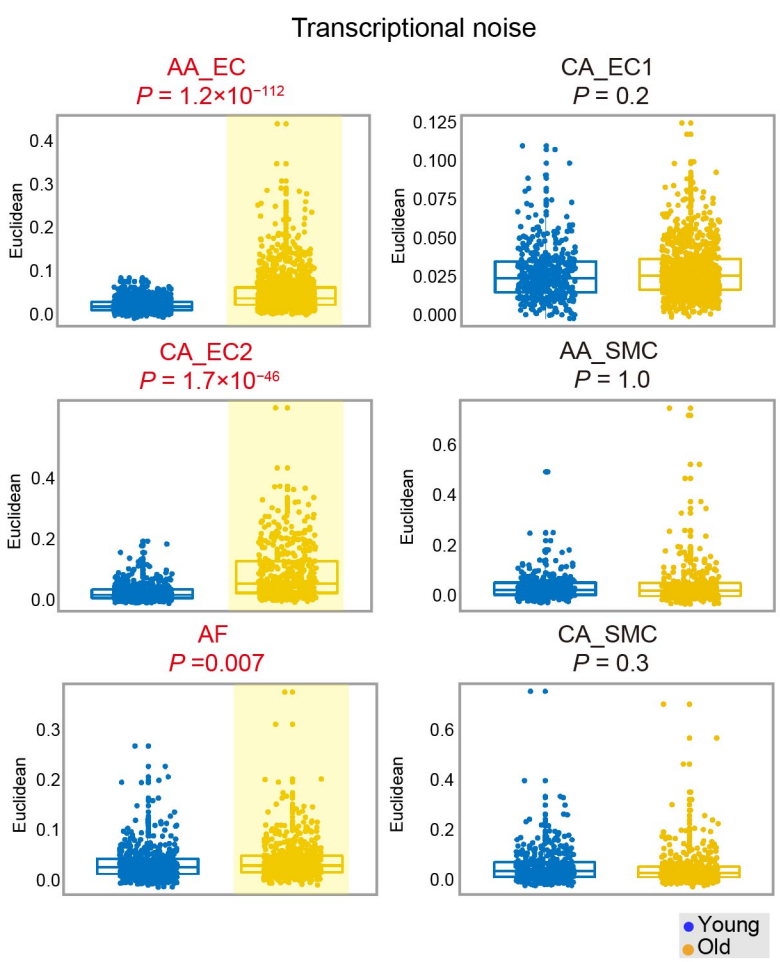


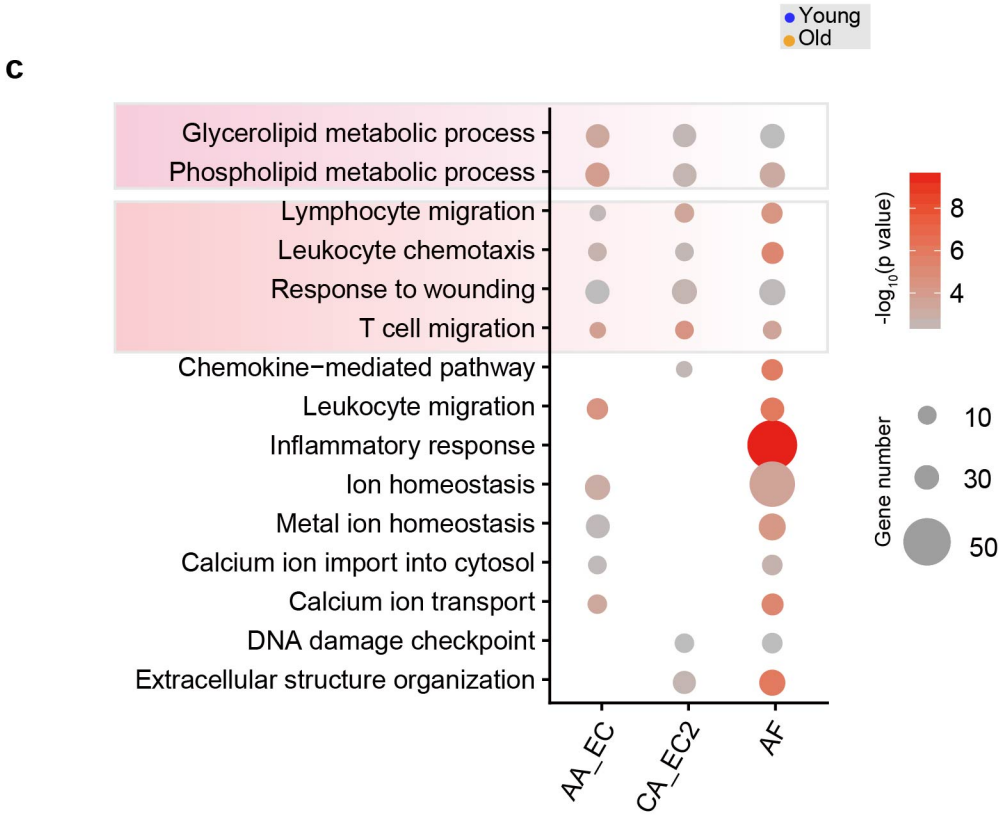

**Supplementary Fig. 7, Transcriptional noise increases in vascular cells from older monkeys.** **a,** Unique pathways enriched in AA_EC, AA_SMC and CA_EC1, CA_SMC, respectively. **b,** The boxplots show transcriptional noise of individual cells for each cell type. Red p-values (Wilcoxon rank sum test) and yellow boxes highlight significant differences between young and old cells concerning transcriptional noise. Cell number, AA_EC=2480, CA_EC1=1271, CA_EC2=993, AA_SMC=667, CA_SMC=858, AF=1161. **c,** GO analysis of highly variable genes in cell types (AA_EC, CA_EC2, AF) with significantly different transcriptional noise between old and young monkeys.

Supplementary Figure 8

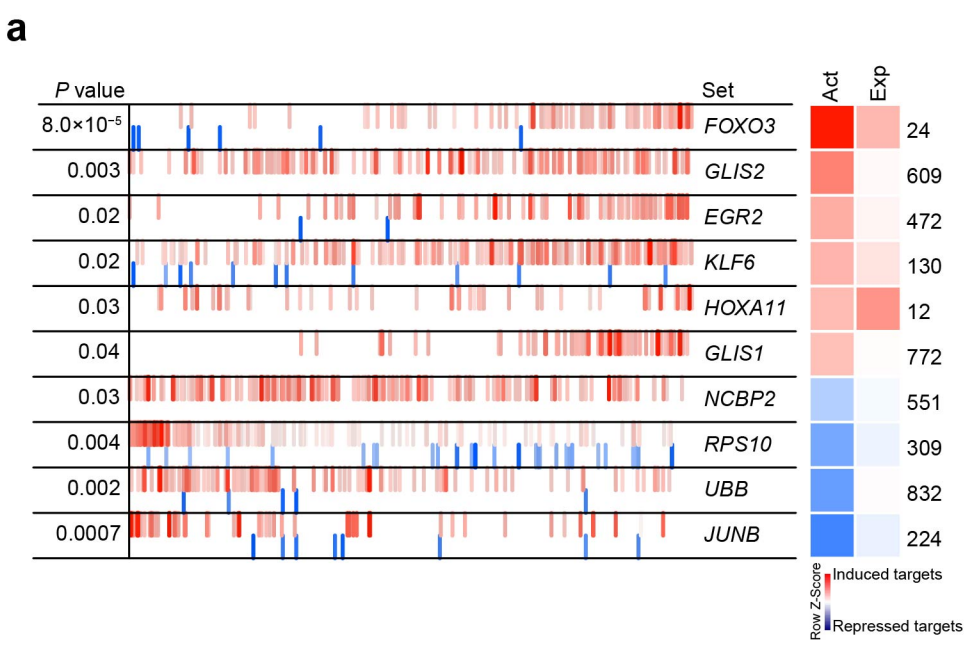


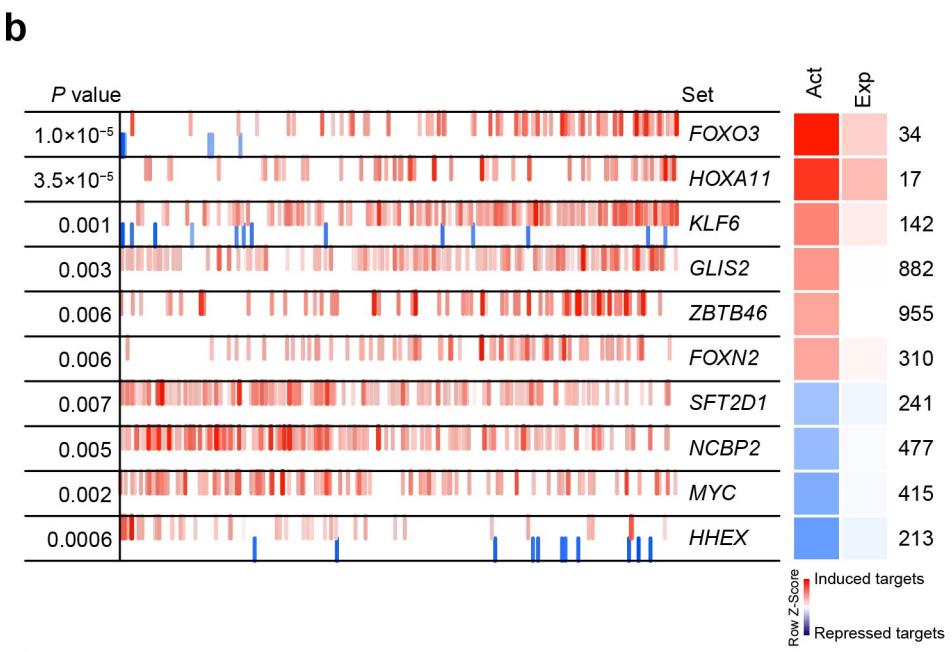


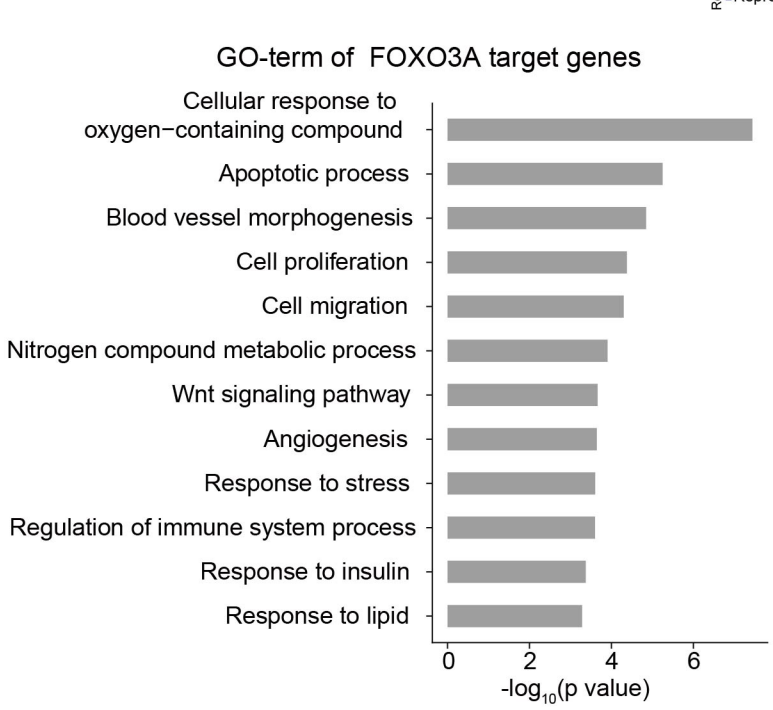


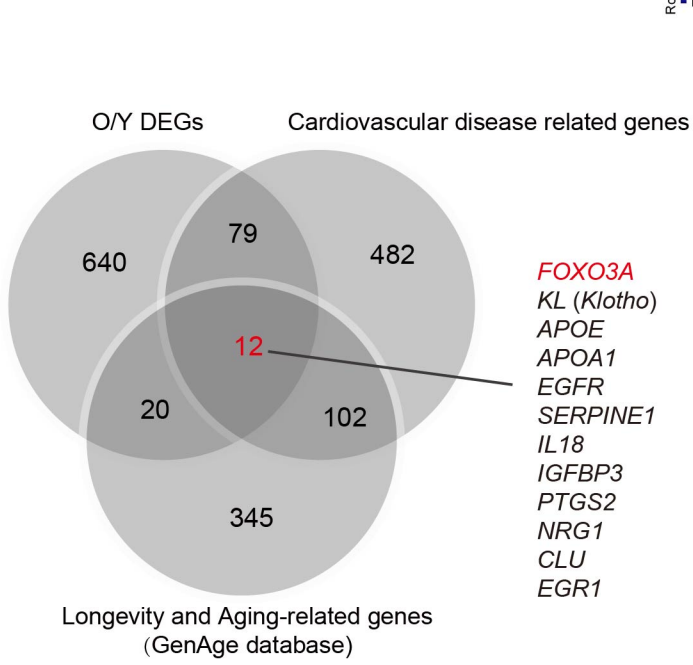


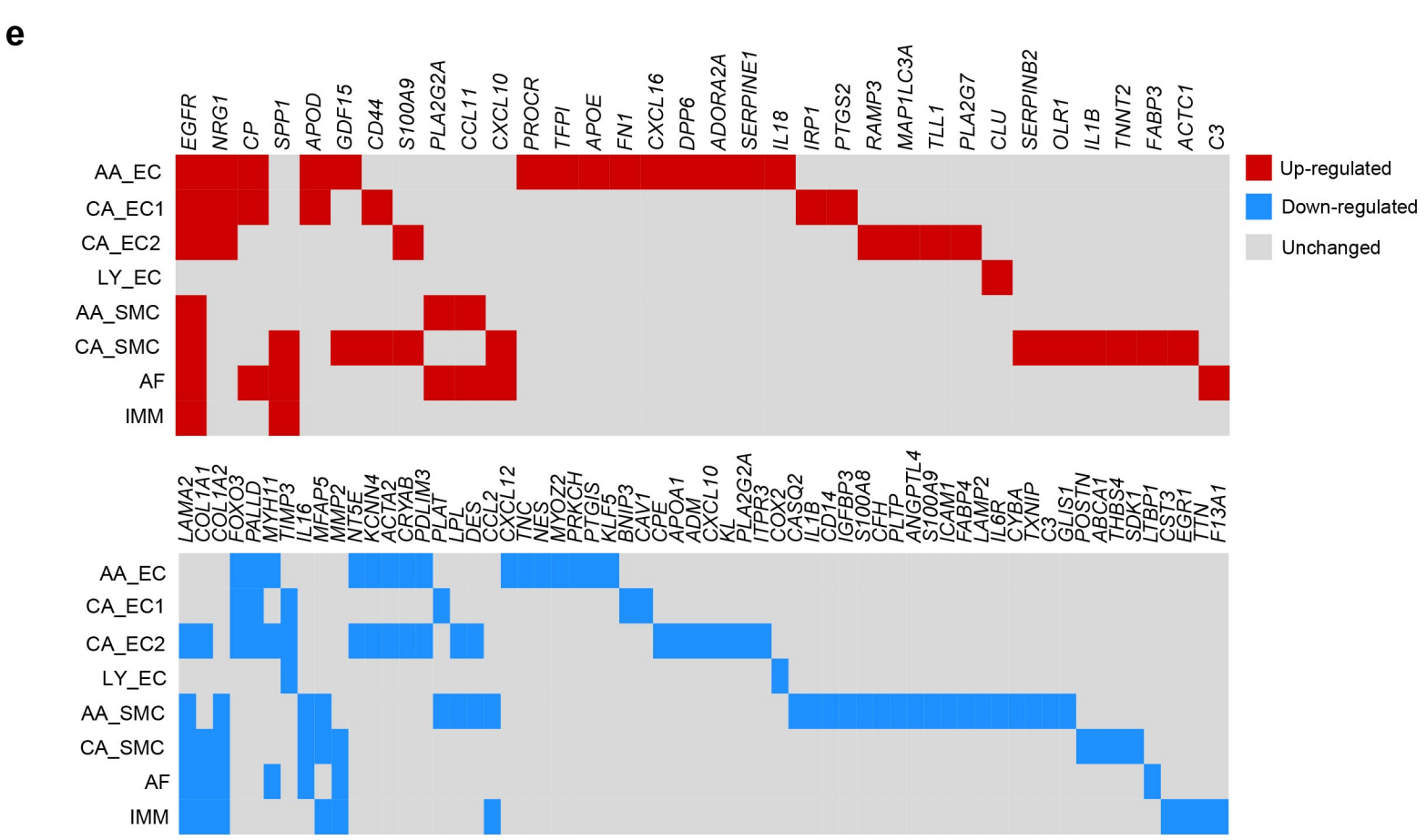


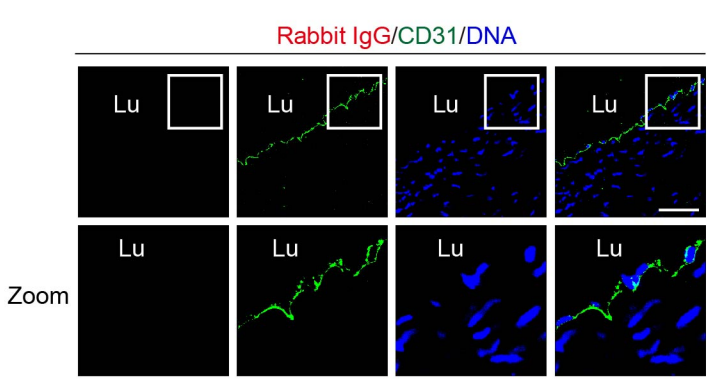

**Supplementary Fig. 8, FOXO3A is at the center of the aging interactome. a-b,** Interactome and master regulators (MRs) inferred by ARACNe and VIPER analysis. All age-related DEGs from different cell types were sorted in order with the largest downregulation (left) and largest upregulation (right) of aging-related genes shown on the x-axis. P-values were calculated by Student's t-test are shown on the left of the heatmap. Different activity (act) of MRs (absolute normalized enrichment score) and different expression (exp) levels of MRs are shown in the heatmap on the right. Numbers on the right indicate the rank of each MR among the DEGs**. a,** Top candidate MRs during aging. n = 7,989 cells, all cell types included. **b,** Top candidate master regulators during aging. n = 4,744 endothelial cells. **c,** Comparisons of GO-enriched terms of FOXO3A targeted O/Y DEGs which were identified by SCENIC. *n* = 7,989 cells. **d,** Venn diagram depicting the overlap between O/Y genes and cardiovascular disease–related and aging/longevity-related gene sets. **e,** Heatmap showing the overlapping cardiovascular disease–related genes with DEGs (O/Y DEGs, Bonferroni-corrected p-value $\leq 0.05$ and $\log_2$ [fold change] $\geq 0.5$) for each cell type from young and old monkeys. Rows are cell types and columns are representative genes. Red, upregulated genes; blue, downregulated genes; gray, genes not differentially expressed. P-values were determined by two-sided Wilcoxon rank-sum tests. **f,** Negative control for FOXO3A staining in the aortic artery. Scale bar = 10 μm.

## Supplementary Figure 9

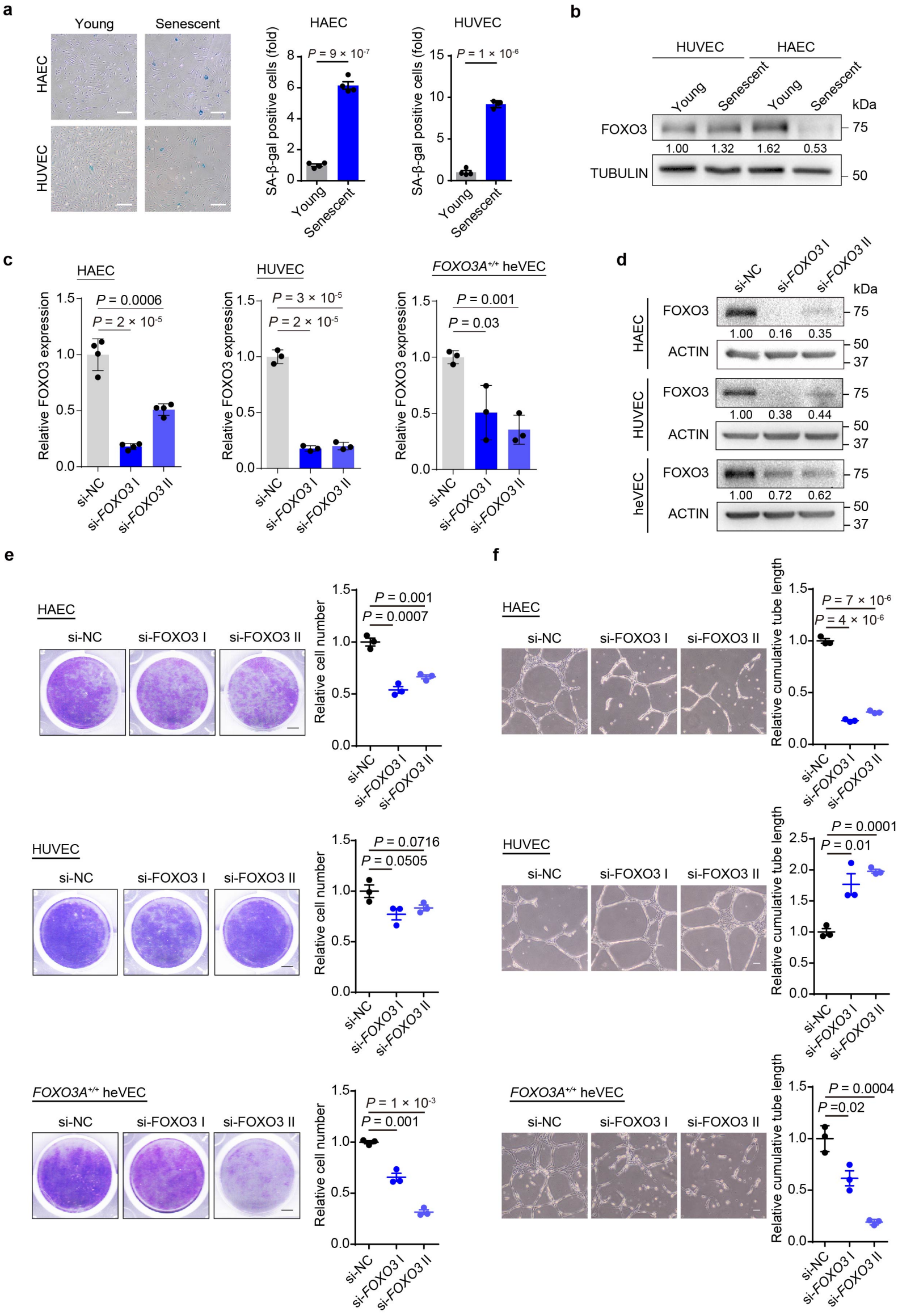

**Supplementary Fig. 9, Silencing FOXO3A activity by siRNA in human aortic endothelial cells (HAECs) and human umbilical vein endothelial cells (HUVECs). a,** Left, SA-β-gal staining of young and senescent HAECs and HUVECs. n = 4 experimental repeats. Scale bar, 25 μm. **b,** Western blotting of FOXO3 protein levels in young and senescent HAECs and HUVECs. **c,** Relative expression level of *FOXO3* in HAECs (P6), HUVECs (P8) and heVECs (P2) derived from hESCs after transfection with siRNAs against *FOXO3* (FOXO3 I and FOXO3 II). n = 3 experimental repeats. **d,** Western blotting of the knockdown efficiency of siRNA-*FOXO3* in HUVECs, HAECs, and heVECs. **e,** Clonal expansion analysis of endothelial cells transfected with siRNAs against *FOXO3*. n = 3 experimental repeats. Scale bar, 100 μm. **f,** *In vitro* angiogenesis, is assessed by the formation of capillary-like tubes from endothelial cells transfected with siRNAs against *FOXO3*. n = 3 experimental repeats. Scale bar, 100 μm. Data are presented as mean ± SEM; p-values were determined by two-sided Student's t-test **(a, c, e, f)**.

## Supplementary Figure 10

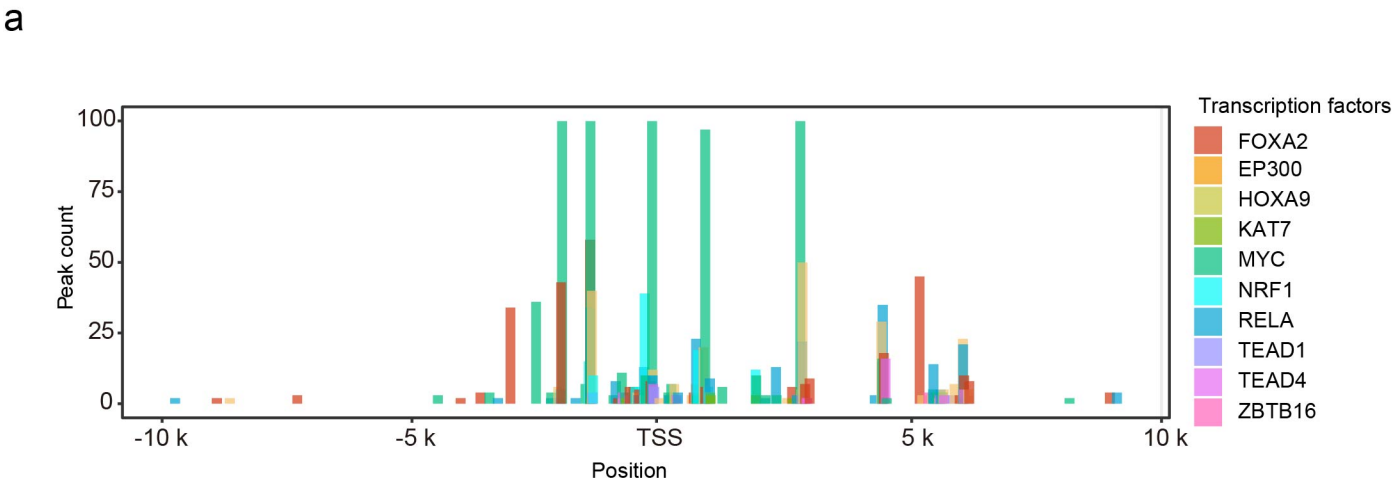


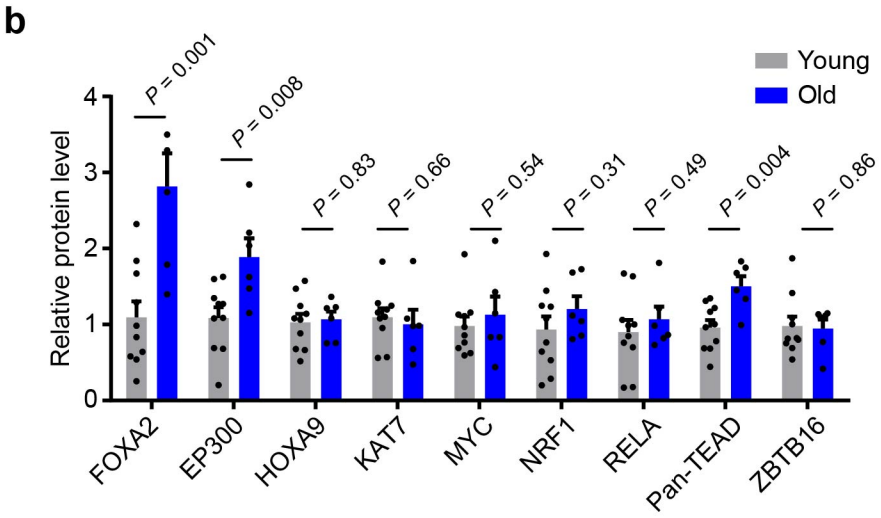


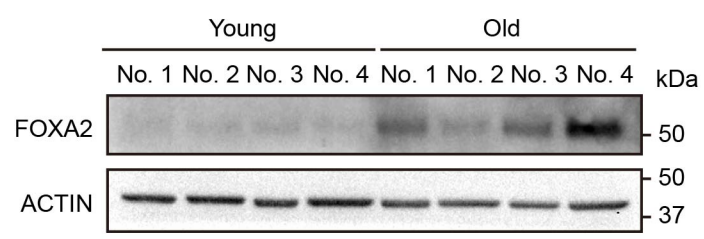


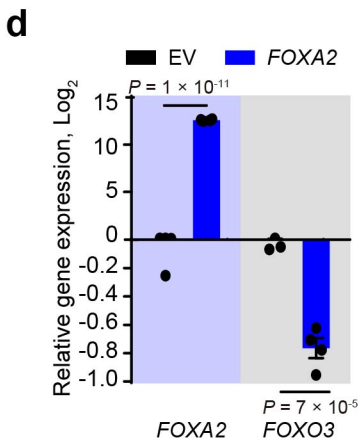


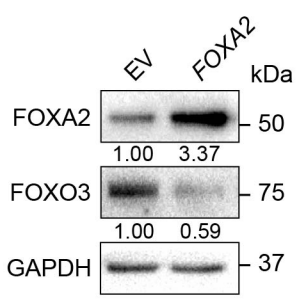


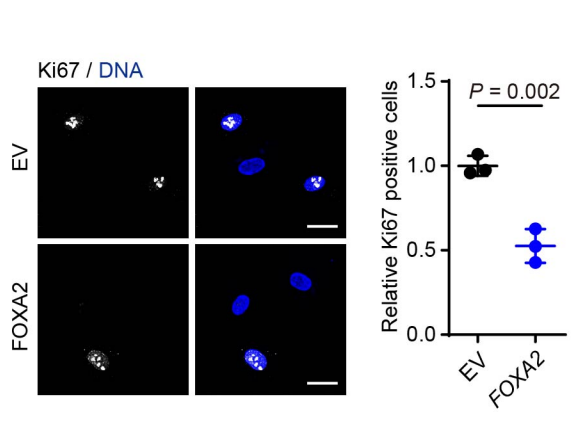


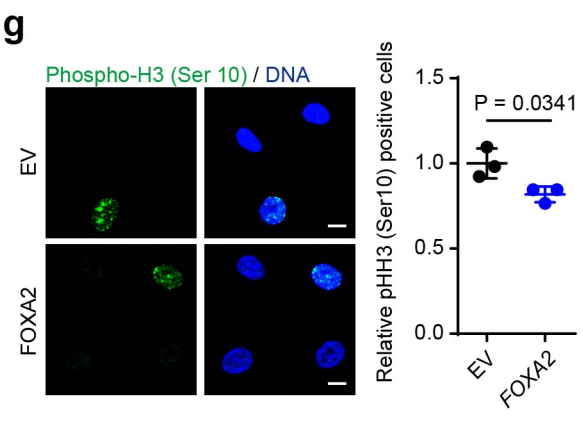


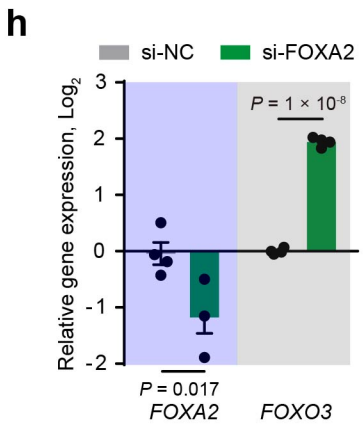


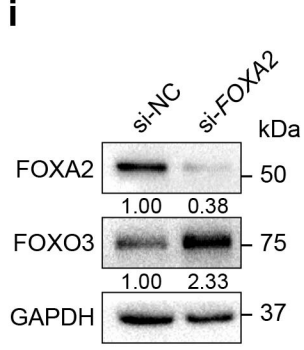


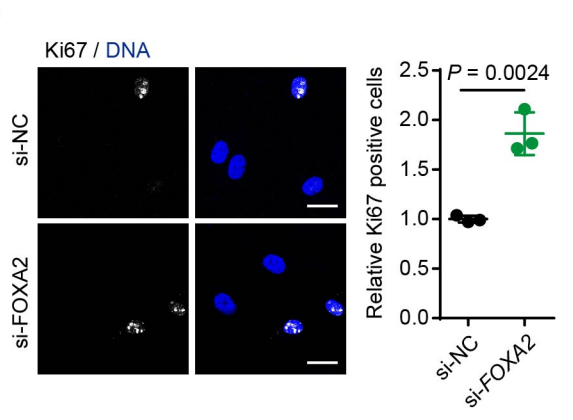


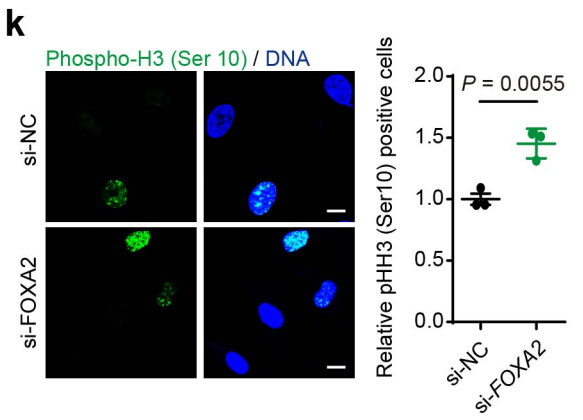


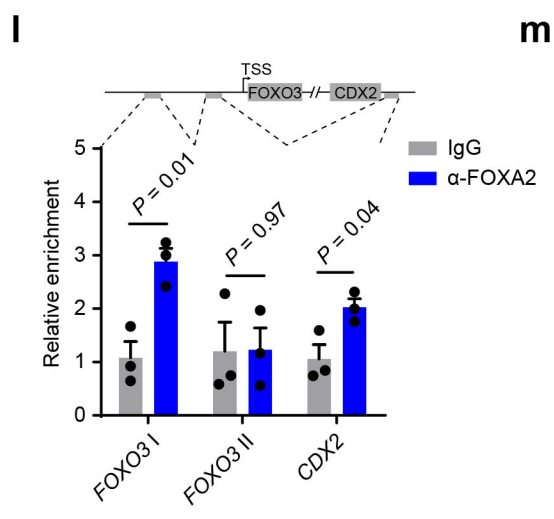


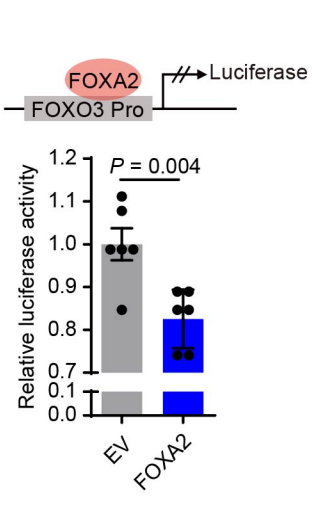


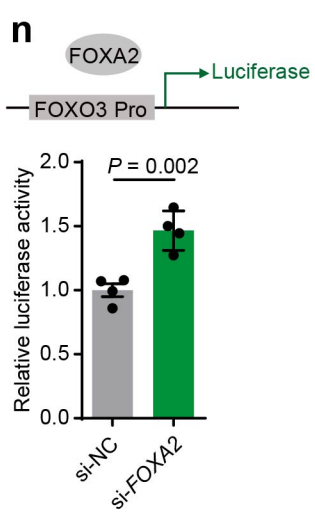

**Supplementary Fig. 10, Identification of FOXA2 as a regulator of FOXO3A. a,** A predicted model for potential regulators of *FOXO3A* (see also method). **b,** The relative contents of potential FOXO3A regulators in indicated samples. n = 8 monkeys. **c,** Western blotting of FOXA2 protein levels in indicated samples. n = 8 monkeys. **d,** RT-qPCR of *FOXA2* and *FOXO3A* in HAECs transfected with vehicle and *FOXA2* expression vectors. n = 4 experimental repeats. **e,** Western blotting of FOXO3 protein in HAECs after overexpressed with *FOXA2*. **f,** Ki67 immunofluorescence staining of HAECs transfected with vehicle or *FOXA2* expression vectors. Scale bar, 25 μm. n = 3 experimental repeats. **g,** Phospho-histone 3 immunofluorescence staining of HAECs transfected with vehicle or *FOXA2* expression vectors. Scale bar, 10 μm. n = 3 experimental repeats. **h,** RT-qPCR of *FOXA2* and *FOXO3A* in HAECs transfected with si-*NC* or si-*FOXA2*. n = 4 experimental repeats. **i,** Western blotting of FOXO3 protein in HAECs transfected with si-NC and si-*FOXA2*. **j,** Ki67 immunofluorescence staining of HAECs transfected with si-NC and si-*FOXA2*. Scale bar, 25 μm. n = 3 experimental repeats. **k,** Phospho-histone 3 immunofluorescence staining of HAECs transfected with si-NC and si-*FOXA2*. n = 3 experimental repeats. Scale bar, 10 μm. **l,** ChIP-qPCR assessment of the enrichment of FOXA2 in the upstream region of *FOXO3A*. *FOXO3* I and *FOXO3* II represent two different regions containing putative FOXA2 binding motifs. *CDX2* is used as a positive control. n = 3 experimental repeats. **m,** Luciferase activity of the *FOXO3A* promoter measured in HAECs transfected with vehicle and *FOXA2* expression vectors. n = 6 experimental repeats. **n,** Luciferase activity of the *FOXO3A* promoter measured in HAECs transfected with si-NC and si-*FOXA2*. n = 4 experimental repeats. Data are presented as mean ± SEM; p-values were determined by two-sided Student's t-test **(b, d, f, g, h, j-n)**.

## Supplementary Figure 11

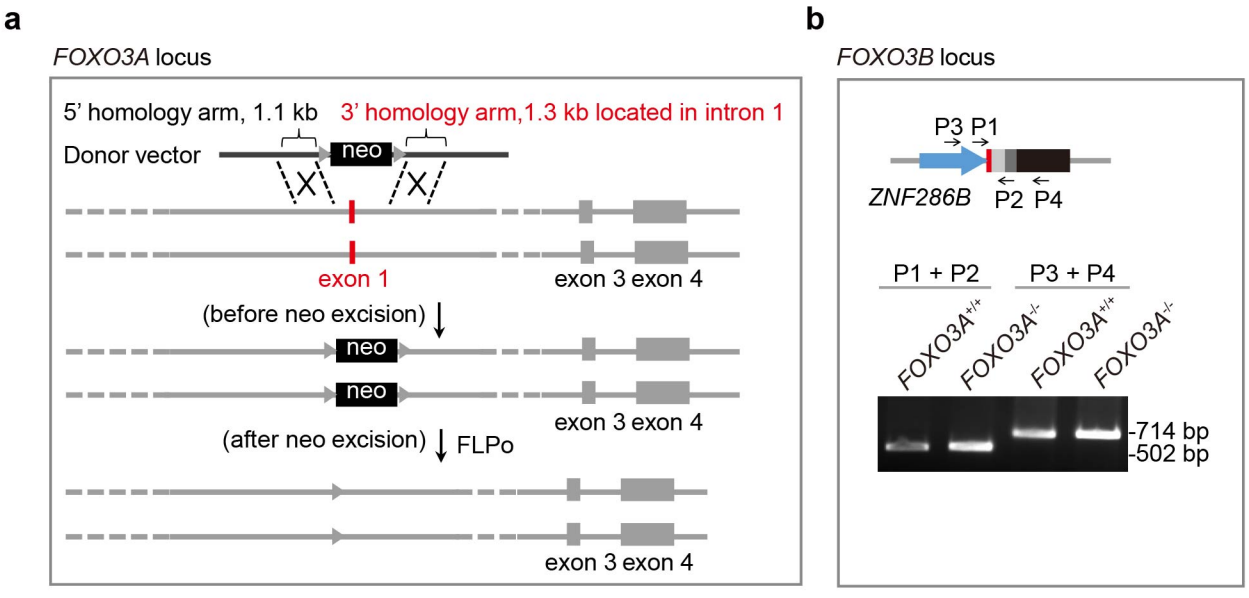


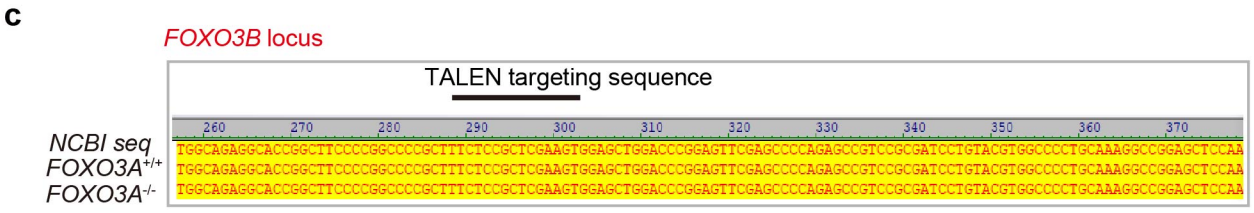


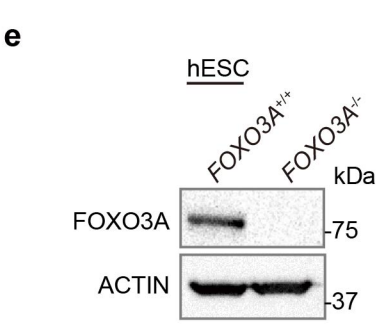


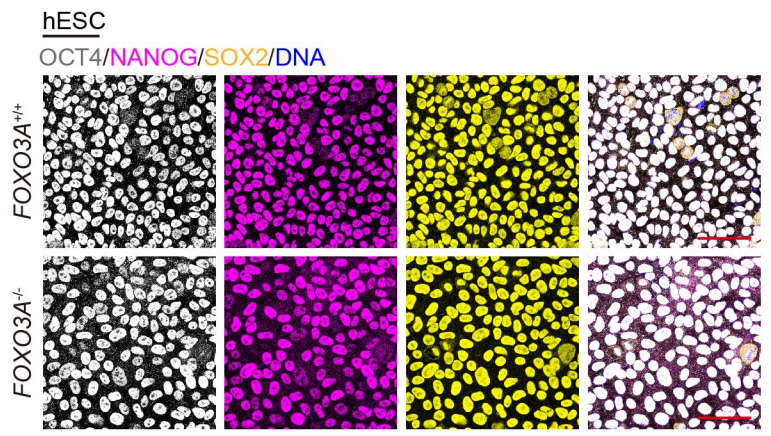


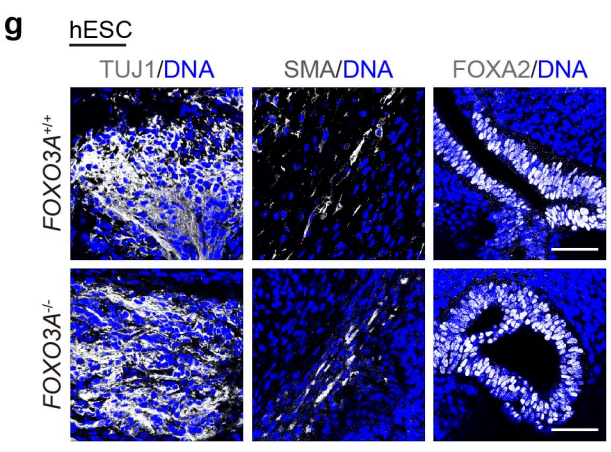


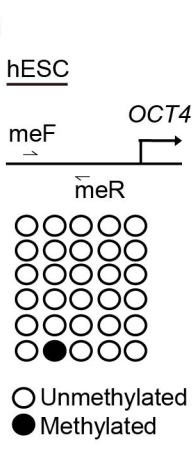


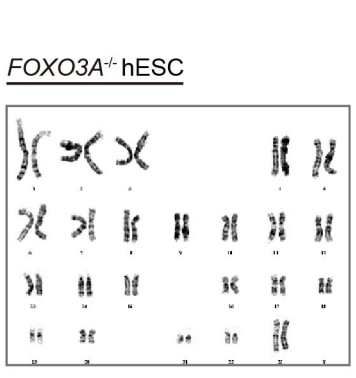

**Supplementary Fig. 11, Characterization of *FOXO3A*$^{-/-}$ hESCs. a,** Schematic representation of *FOXO3*A knockout in hESCs by TALEN-mediated gene targeting technique. Exon 1 of *FOXO3A* was removed. **b,** TALEN-facilitated homologous recombination was used to specifically knock out *FOXO3A* without affecting *FOXO3B*. PCR of the *FOXO3B* gene from the wild-type and *FOXO3A*$^{-/-}$ cell genomes using primer pairs P1/P2 or P3/P4. The *FOXO3B* locus remains intact in *FOXO3A*$^{-/-}$ cells. **c,** Genomic sequencing of the *FOXO3B* gene. **d**, Sequencing of the TALEN-targeted regions in the *FOXO3B* or *FOXO3A* gene. The y-axes show the coverage of detected sequences in wild-type and *FOXO3A*$^{-/-}$ cells. The red area, missing sequencing in the *FOXO3A* region. **e**, Western blotting of FOXO3A protein levels in *FOXO3A*$^{+/+}$ and *FOXO3A*$^{-/-}$ hESCs. **f,** Immunofluorescence analysis indicating the expression of three pluripotency markers in wild-type and *FOXO3A*-deficient hESCs. Scale bar, 50 μm. **g,** Immunostaining images showing *in vivo* differentiation potential to ectodermal (TUJ1), mesodermal (SMA) and endodermal (FOXA2) tissues in teratomas derived from *FOXO3A*-deficient hESCs. Scale bar, 50 μm. **h,** DNA methylation status of the *OCT4* promoter in *FOXO3A*$^{-/-}$ hESCs. **i,** Karyotyping analysis of *FOXO3A*-deficient hESCs indicating normal karyotype.

## Supplementary Figure 12

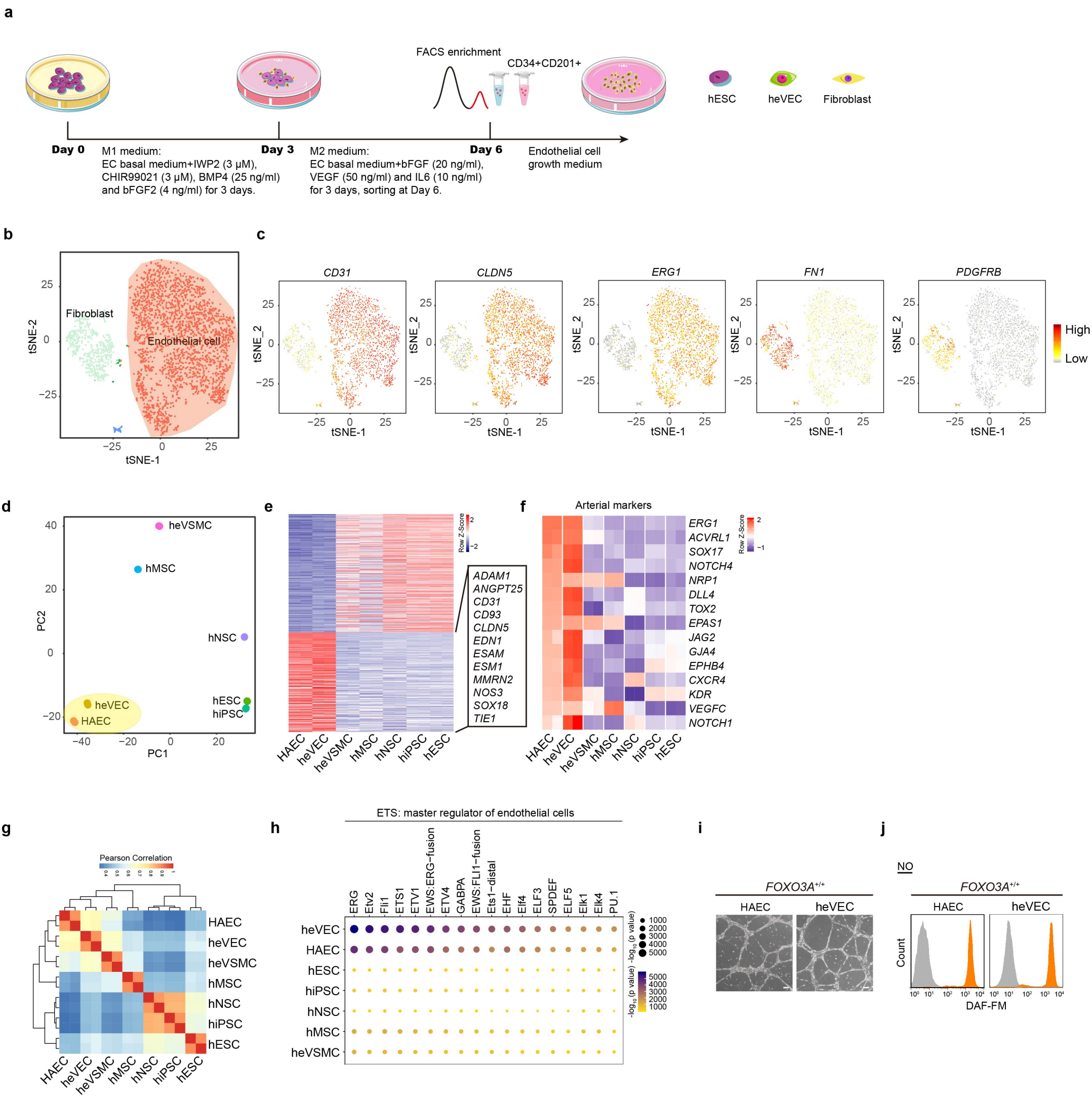

**Supplementary Fig. 12, Optimized protocol for endothelial cell differentiation. a,** Schematic showing the method used to generate heVECs from hESCs. **b,** Single cell sequencing of heVECs differentiated from hESCs. **c,** Cell-type expression signatures. (gray, no expression; dark red, relatively higher expression). **d,** Principle component analysis (PCA) of the various cell populations. heVEC, hNSC, hMSC, heVSMC are human vascular endothelial cell, neural stem cell, mesenchymal stem cell, and vascular smooth cells differentiated from hESCs (human embryonic stem cells). iPSCs, induced pluripotent stem cells, HAECs, primary aortic endothelial cells. **e,** Heatmap showing DEGs between endothelial cells and other cell lines, with endothelial marks are specifically expressed in both of HAECs and heVECs. **f,** Heatmap showing arterial endothelial cell specific gene expression expressed in both of HAECs and heVECs. **g,** The Pearson correlation analysis of ATAC-seq atlas from various cell types. **h,** Endothelial cells specifically enriched TF motifs from ATAC-seq analysis. **i,** *In vitro* angiogenesis, is assessed by the formation of capillary-like tubes. Scale bar, 100 μm. **j,** FACS analysis to test nitric oxide (NO) production of endothelial cells. For measurement of nitric oxide (NO), about $5\times10^5$ HAECs and heVECs were treated with DAF-FM (Molecular Probes, Invitrogen) for 30 mins at room temperature. After staining, cells were analyzed by FACS.

## Supplementary Figure 13

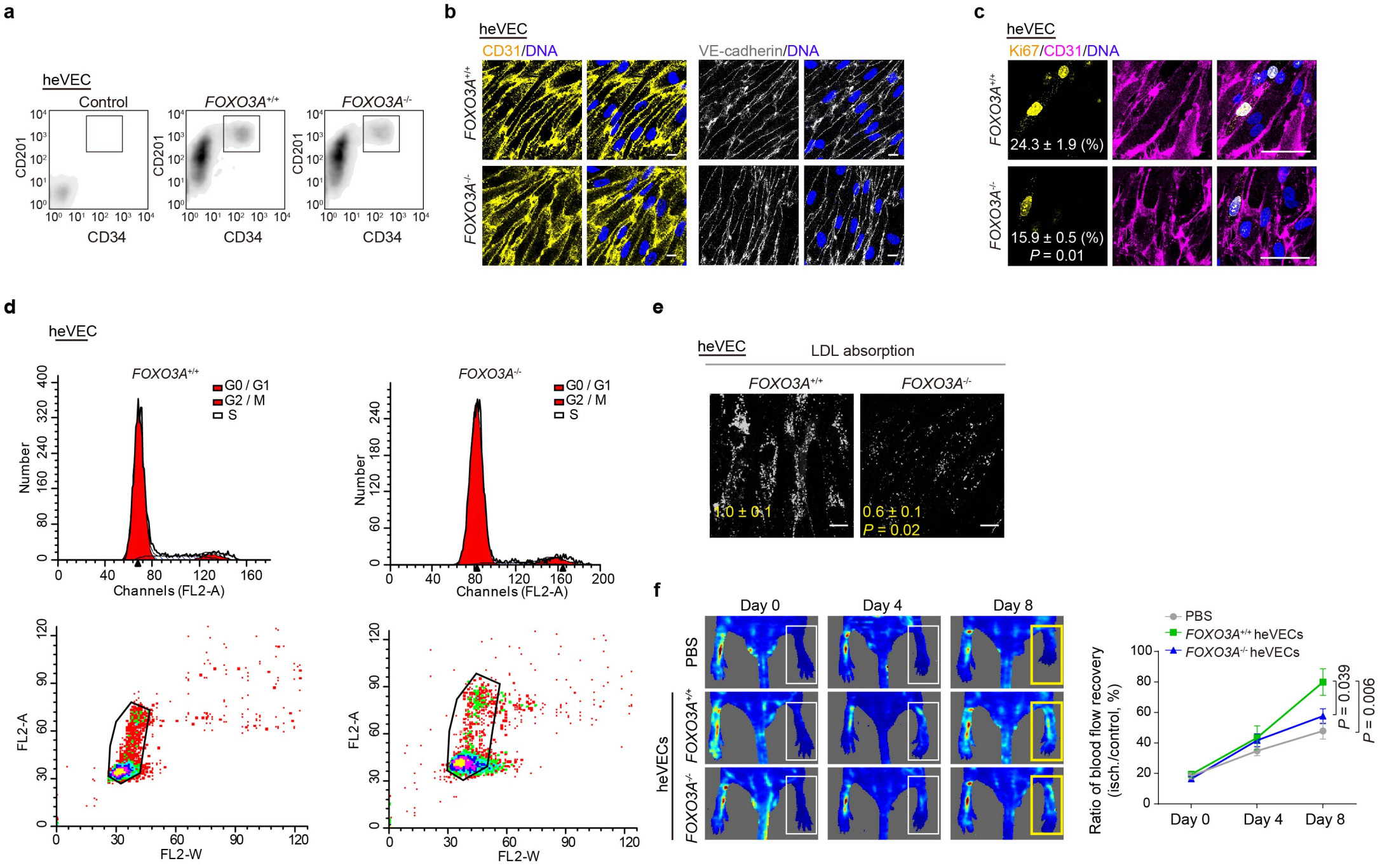

**Supplementary Fig. 13, Characterization of *FOXO3A*$^{-/-}$ heVECs.** **a,** FACS enrichment of heVECs. **b,** Immunostaining for CD31 and VE-cadherin in *FOXO3A*$^{+/+}$ and *FOXO3A*$^{-/-}$ heVECs. Scale bar, 10 μm. **c,** Representative Ki67 and CD31 immunofluorescence staining of *FOXO3A*$^{+/+}$ and *FOXO3A*$^{-/-}$ heVECs. Numbers represent the percentage of Ki67-positive cells under each condition. n = 3 experimental repeats. Scale bar, 50 μm. **d,** The raw data of FACS analysis of cell cycle of *FOXO3A*$^{+/+}$ and *FOXO3*$^{-/-}$ heVECs. **e,** Uptake of acetylated low-density lipoprotein (Ac-LDL) by *FOXO3A*$^{+/+}$ and *FOXO3A*$^{-/-}$ heVECs. Numbers represent the relative immunofluorescence intensity of Ac-LDL under each condition. n = 3 experimental repeats. Scale bar, 10 μm. **f,** Blood flow recovery kinetics of each hindlimb ischemic mouse (n = 10) after transplantation of PBS, *FOXO3A*$^{+/+}$ and *FOXO3A*$^{-/-}$ heVECs, separately. Data are the mean ± SEM; p-values were determined by two-tailed Student's t-test (**c, e, f**).

## Supplementary Figure 14

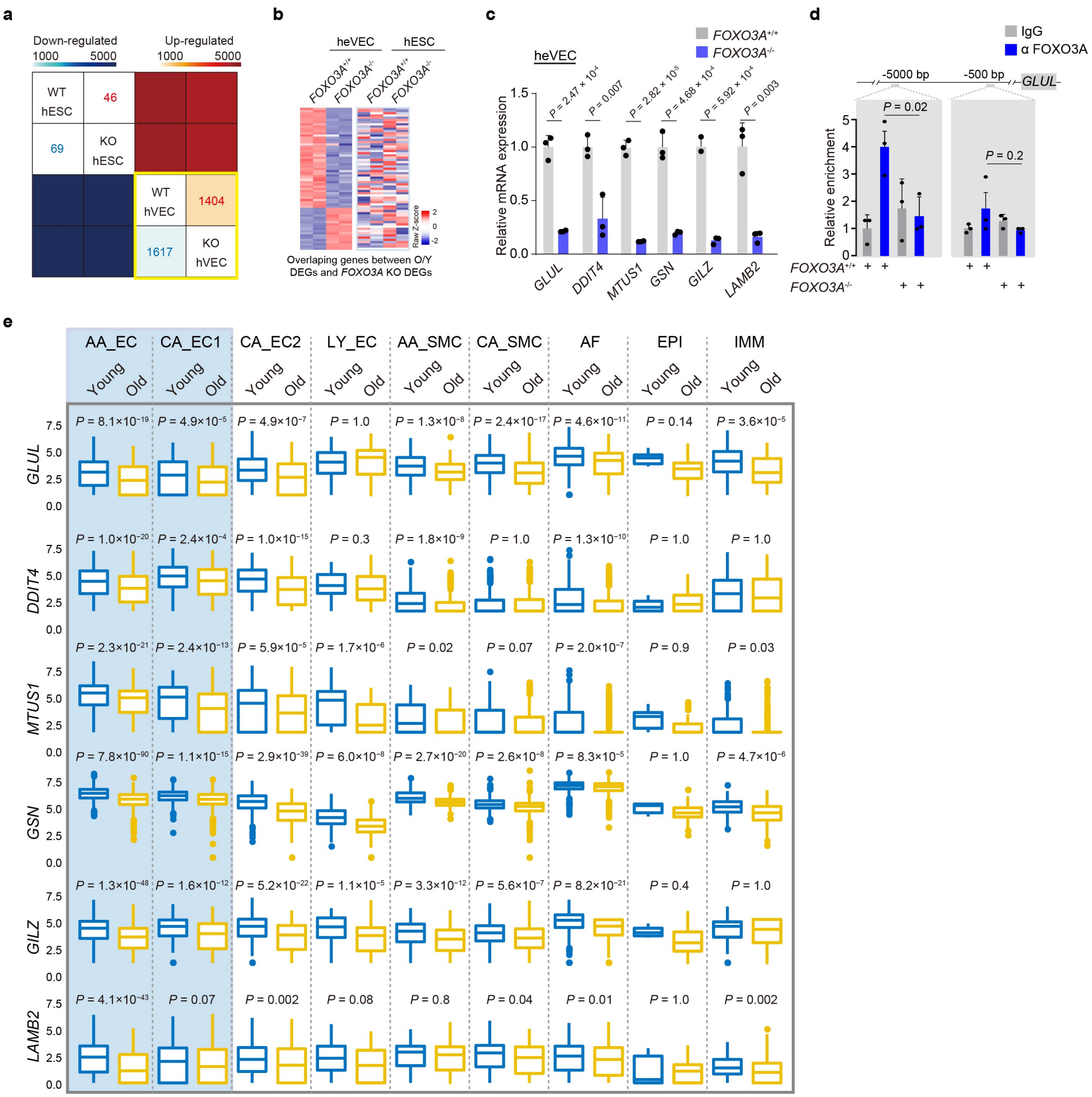

**Supplementary Fig. 14, Transcriptomic profiling of *FOXO3A* deficient human vascular cells.** **a,** Heatmap showing the number of differentially expressed genes (DEGs) in WT and *FOXO3A*-deficient hESCs and heVECs. WT stands for wild-type, KO stands for knockout of *FOXO3A*. **b,** Heatmap of 64 common genes overlapped between O/Y DEGs of aged monkey EC and *FOXO3A* KO DEGs of heVECs. These genes were specific upregulated or downregulated in *FOXO3A* deficient heVECs, but not *FOXO3A* deficient heVECs when compared to wildtype heVECs and wildtype ESCs, respectively. **c,** RT-qPCR of indicated genes in heVECs. n = 3 experimental repeats. **d,** ChIP-qPCR assessment of the enrichment of FOXO3A in the upstream region of *GLUL*. n = 3 experimental repeats. **e,** Box plots inside showing the expression of the indicated genes across cell types, p-values were determined by Wilcoxon rank sum test. Data are presented as mean ± SEM; p-values were determined by two-sided Student's t-test (**c, d, e**).

## Supplementary Figure 15

**a**

Fig. 3h

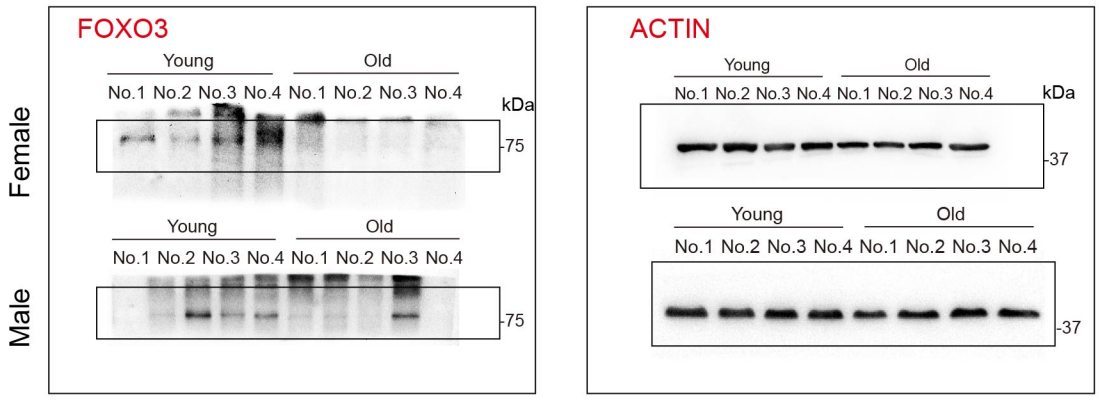


**b**

Supplementary Fig. 9b

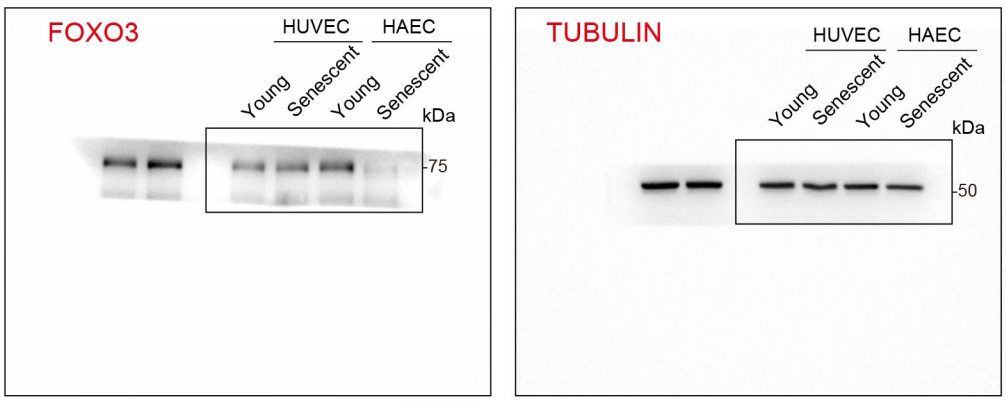


**c**

Supplementary Fig. 9d

HAEC

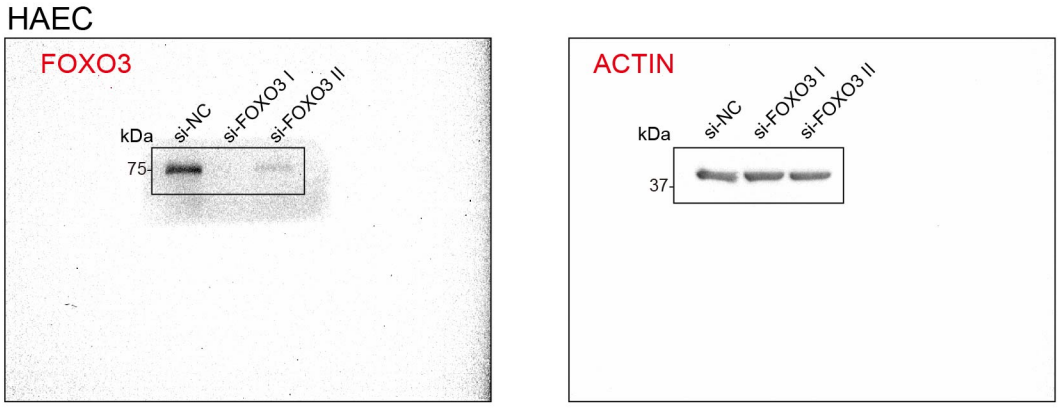


HUVEC

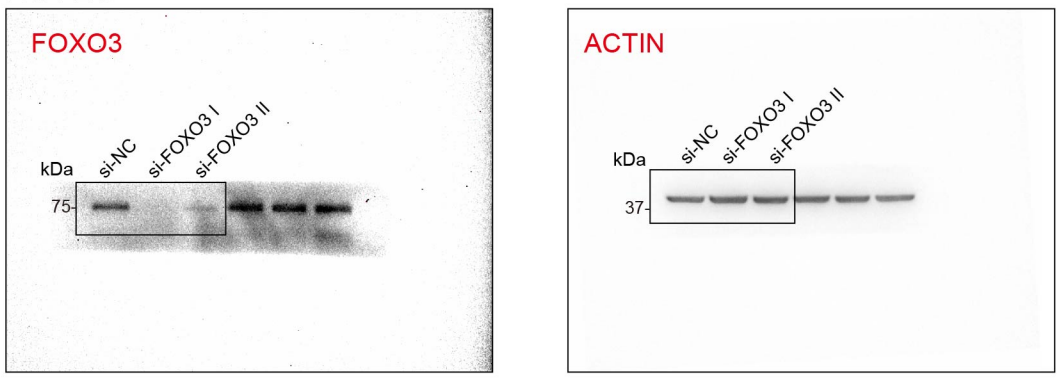


heVEC

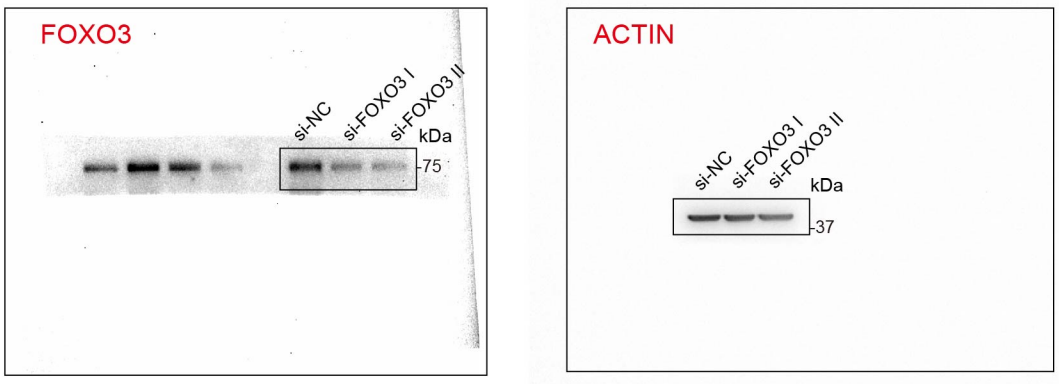

**Supplementary Fig. 15, Uncropped scans of gels and western blots.** (a-c) Uncropped blots of Fig. 3h and Supplementary Figs. 9b and 9d. Edited blots or gels were marked by black rectangles.

## Supplementary Figure 16

**a**

Supplementary Fig. 10c

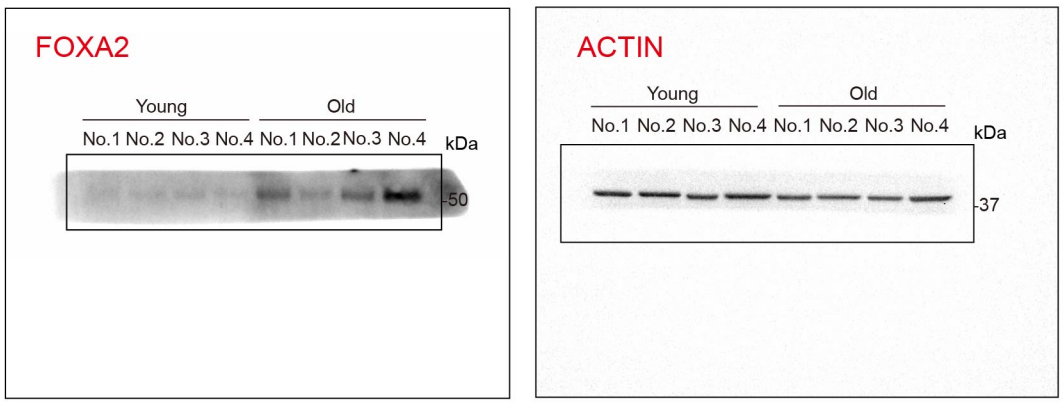


**b**

Supplementary Fig. 10e

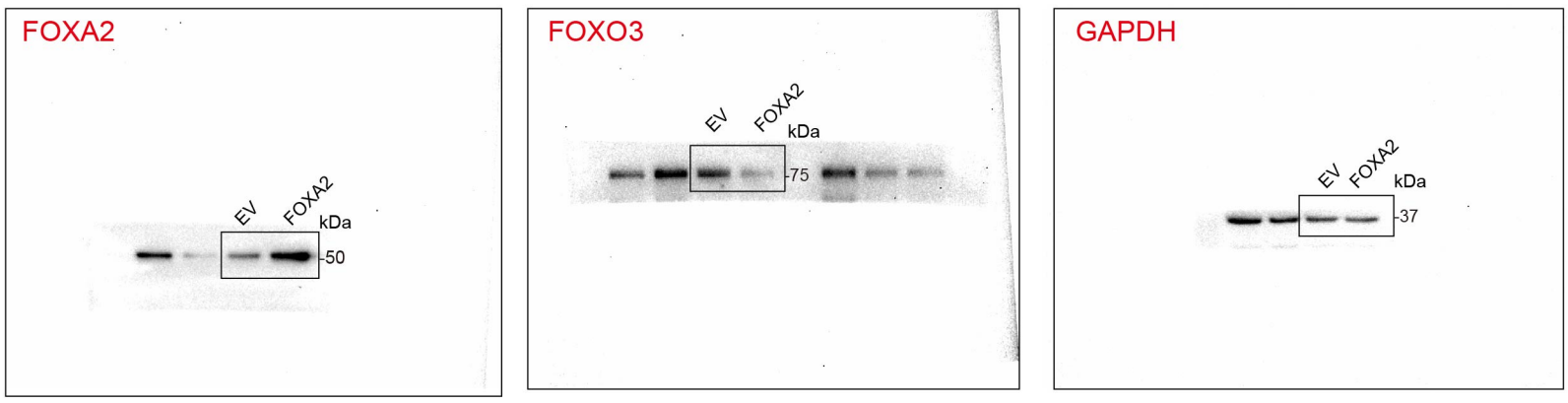


**c**

Supplementary Fig. 10i

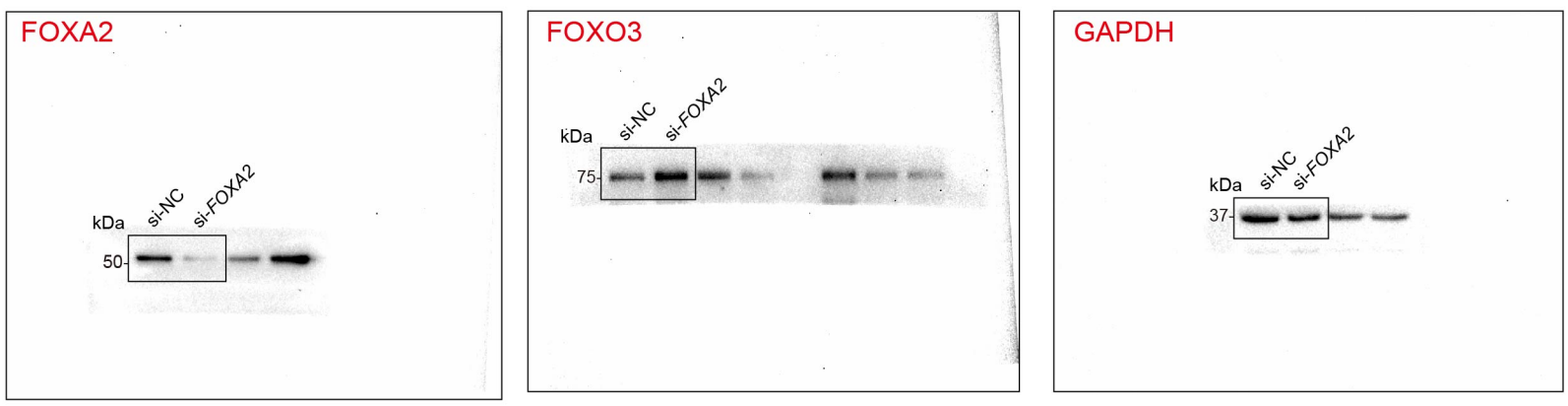


**d**

Supplementary Fig. 11b

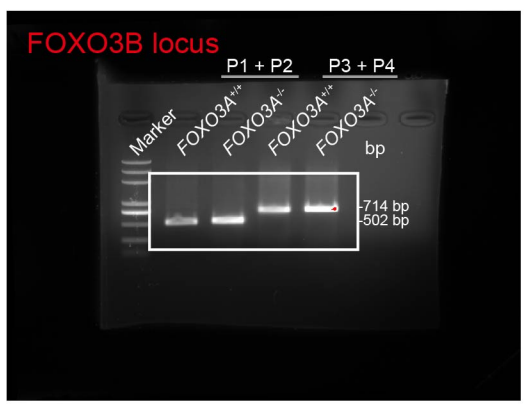


**e**

Supplementary Fig. 11e

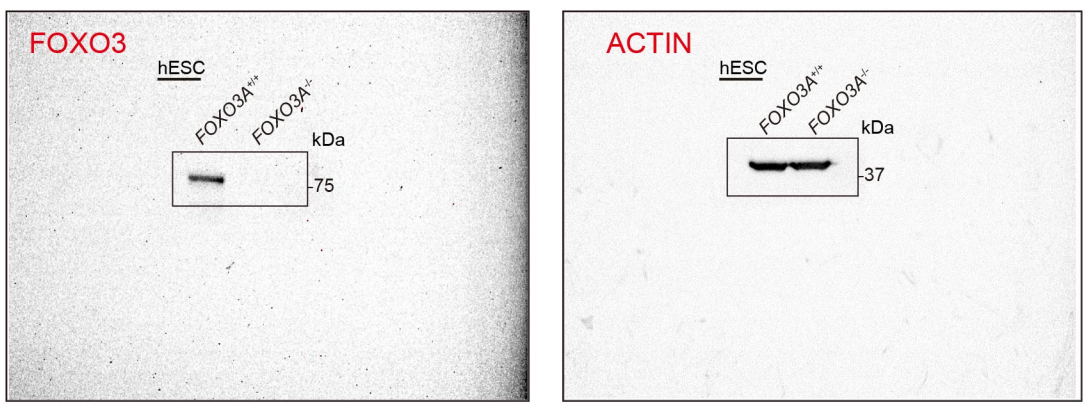

**Supplementary Fig 16, Uncropped scans of gels and western blots.** (a-e) Uncropped blots of Supplementary Figs. 10c, 10e, 10i, 11b and 11e. Edited blots or gels were marked by black rectangles.